J. Membrane Biol. 198, 103–112 (2004)
DOI: 10.1007/s00232-004-0664-0

The Journal of
Membrane
Biology



# Rate-limiting Reactions Determining Different Activation Kinetics of Kv1.2 and Kv2.1 Channels

**A. Scholle[1], S. Dugarmaa[1], T. Zimmer[1], M. Leonhardt[1], R. Koopmann[1], B. Engeland[2], O. Pongs[2], K. Benndorf[1]**

[1]Institut für Physiologie, Herz-Kreislauf-Physiologie, Friedrich-Schiller-Universität, 07740, Jena, Germany
[2]Zentrum für Molekulare Neurobiologie, Institut für Neurale Signalverarbeitung, UKE (Haus 42), Martinistr. 52, 20251, Hamburg, Germany

Received: 26 August 2003/Revised: 5 February 2004

**Abstract.** To identify the mechanisms underlying the faster activation kinetics in Kv1.2 channels compared to Kv2.1 channels, ionic and gating currents were studied in rat Kv1.2 and human Kv2.1 channels heterologously expressed in mammalian cells. At all voltages the time course of the ionic currents could be described by an initial sigmoidal and a subsequent exponential component and both components were faster in Kv1.2 than in Kv2.1 channels. In Kv1.2 channels, the activation time course was more sigmoid at more depolarized potentials, whereas in Kv2.1 channels it was somewhat less sigmoid at more depolarized potentials. In contrast to the ionic currents, the ON gating currents were similarly fast for both channels. The main portion of the measured ON gating charge moved before the ionic currents were activated. The equivalent gating charge of Kv1.2 ionic currents was twice that of Kv2.1 ionic currents, whereas that of Kv1.2 ON gating currents was smaller than that of Kv2.1 ON gating currents. In conclusion, the different activation kinetics of Kv1.2 and Kv2.1 channels are caused by rate-limiting reactions that follow the charge movement recorded from the gating currents. In Kv1.2 channels, the reaction coupling the voltage-sensor movement to the pore opening contributes to rate limitation in a voltage-dependent fashion, whereas in Kv2.1 channels, activation is additionally rate-limited by a slow reaction in the subunit gating.

**Key words:** Kv2.1 and Kv1.2 channels — Equivalent gating charge — Ionic and gating current — Activation time course — Voltage dependence

*Correspondence to:* K. Benndorf; email: kben@mti-n.uni-jena.de

## Introduction

Four α subunits of voltage-dependent $K^+$ (Kv) channels assemble to constitute functional channels (MacKinnon, 1991; Heginbotham & MacKinnon, 1992; Liman, Tytgat & Hess, 1992). The voltage is sensed by transmembrane domains that move charge across the membrane. This charge can be determined by measuring gating currents. The main element of the voltage sensor is the S4 segment (Liman et al., 1991; Papazian et al., 1991; Logothetis et al., 1992; Perozo et al., 1994; Larsson et al., 1996; Cha & Bezanilla, 1998) that moves in an outward direction in response to depolarization (Larsson et al., 1996, Yusaf, Wray & Sivaprasadarao, 1996; Starace, Stefani & Bezanilla, 1997; Cha & Bezanilla, 1997). The S4 segment contains between four and eight positively charged amino acids, of which, however, only a fraction is involved in the gating (Aggarwal & MacKinnon, 1996; Seoh et al., 1996). Negatively charged residues in the S2 and S3 segment were also identified to contribute to voltage sensing (Papazian et al., 1995; Planells-Cases et al., 1995; Seoh et al., 1996; Tiwari-Woodruff et al., 1997, Cha & Bezanilla, 1997; Milligan & Wray, 2000). Very recently the crystal structure of a bacterial voltage-gated $K^+$ channel has been reported (Jiang et al., 2003a), confirming essential contribution of the S2, S3, and S4 segments to the voltage sensor. According to the crystal structure, the N-terminal half of S4 and part of S3 (S3b) form a voltage-sensor paddle that may move through the hydrophobic core of the phospholipid membrane upon depolarization, whereas the acidic amino acids of the S2 helices were proposed to stabilize positive paddle charges (Jiang et al., 2003b). It is therefore conceivable that the movement of a similar voltage-sensor paddle gener-

ates the main portion of the gating current in *Shaker* channels. A short initial rising phase in the ON gating currents (Bezanilla et al., 1991; Stefani et al., 1994; Wang et al., 1999; Taglialatela & Stefani, 1993) shows that at least two rate-limiting transitions are involved (for review, *see* Bezanilla, 2000). The coupling between the movement of the voltage sensor and the opening of the pore is less well understood (for review, *see* Yellen, 2002). For *Shaker* channels the extracellular part of the S4 segment of the voltage sensor has been hypothesized to control directly the selectivity filter gate (Elinder, Manniko & Larsson, 2001). For structurally related HERG channels, it has been proposed that movement of the S4 segment triggers an association between the S4–S5 linker and the S6 activation gate (Sanguinetti & Xu, 1999; Tristani-Firouzi, Chen & Sanguinetti, 2002). Furthermore, for *Shaker* and hyperpolarization-activated, cyclic-nucleotide gated (HCN) channels, an involvement of the S4–S5 linker in the coupling process was shown (McCormack et al., 1991; Shieh, Klemig & Kirsch, 1997; Chen et al., 2001). The latter view of the coupling process is supported by the recent structural data, which suggest that movement of the voltage-sensor induces movement of the S4–S5 linker, which in turn moves the S5 helices and the pore, resulting in channel opening (Jiang et al., 2003a, b).

Despite this enormously grown insight into the structure and function of voltage-gated $K^+$ channels over the last years, many questions remain unanswered (Cohen, Grabe & Jan, 2003), among these the question why highly homologous channels activate with different kinetics. In previous studies we addressed the question why Kv1.2 channels activate approximately three times faster than Kv2.1 channels (Scholle et al., 2000; Koopmann et al., 2001). By studying chimeras between Kv1.2 and Kv2.1 channels, we showed that the S4 segment, the S5-pore linker, and the pore itself contribute to the observed difference in the activation time courses of Kv1.2 and Kv2.1 channels. In the present study, the activation gating of Kv1.2 and Kv2.1 channels is analyzed in order to identify at which stage of the activation process the characteristic kinetic difference is determined. We show that the initial gating, measured by the gating current, has a similar time course in both channels and that the characteristic differences in the activation time course are generated by different reactions following the initial charge movement.

## Materials and Methods

### Heterologous Expression Experiments

The cDNA sequence of human Kv2.1 (accession X68302) was subcloned into the *Asp*718I/*Pst*I site of the mammalian expression vector pTracerSV40 (Invitrogen), a vector that allows the simultaneous expression of the green fluorescent protein (GFP) in a second expression cassette and thus the selection of transfected cells upon excitation of GFP. The sequences of rat Kv1.2 (accession X16003) was subcloned into the *Hind*III/*Eco*RI site of pTracerSV40G, a derivative of pTracerSV40 that was obtained by an exchange of the coding region of GFP by that of the enhanced GFP variant (EGFP) from Clontech. Plasmids were amplified in *Escherichia coli* strain DH5α and purified using the EndoFree Plasmid Maxi Kit from Qiagen (Hilden, Germany). Chinese hamster ovary (CHO) cells and the mouse fibroblast cell line (L cells) were transfected using the Effectene reagent from Qiagen. Optimization of the transfection method was done according to the recommendations of the supplier, resulting in the following transfection mixture: 1 μg purified plasmid DNA, 150 μl buffer EC, 8 μl enhancer reagent, and 25 μl Effectene in 2 ml growth medium (per 50 mm dish). The transfection mixture was removed after an incubation of 18 to 20 h. Cells were trypsinized, washed with PBS, resuspended in fresh growth medium and aliquoted into sterile 1.5 ml tubes.

### Electrophysiology

Whole-cell recording was carried out in an experimental chamber (volume ~0.3 ml) mounted on the stage of an inverted microscope (Axiovert 100, Carl Zeiss Jena, Germany) with a conventional patch-clamp technique. The patch-clamp amplifier Axopatch 200B (Axon Instruments, Foster City, CA) was used. The experiments were controlled by a PC using the ISO2 software (MFK, Niedernhausen, Germany). The recording band width was 10 kHz (4-pole Bessel) and was further filtered off-line. The sampling rate was 20 kHz. The patch pipettes were pulled from borosilicate glass. After heat-polishing the resistance was 0.8–2.0 MΩ when filled with one of the pipette solutions (*see* below). A small amount of cell suspension was transferred to the experimental chamber. After settling of the cells, the experimental chamber was perfused for at least five minutes with the final bath solution. An appropriate cell was visually selected by fluorescence of the GFP when excited with UV light. After seal formation and whole-cell access, the series resistance was compensated according to the protocol described in the manual of the amplifier leaving approximately 20% of the series resistance uncompensated.

To measure ionic currents, the pipette solution contained (mM) KCl 120.0, HEPES 10.0, EGTA 5.0, $MgCl_2$ 1.0, pH = 7.20 with KOH, and the bath solution contained NaCl 130.0, HEPES 10.0, KC1 4, $CaCl_2$ 1.8, $MgCl_2$ 1.0, glucose 10.0, pH = 7.35 with NaOH. For measuring gating currents, the pipette solution contained (mM) N-methyl-D-glucamin$^+$ 140, HEPES 10.0, EGTA 5.0, $MgCl_2$ 1.0, pH = 7.20 with HC1, and the bath solution contained N-methyl-D-glucamin$^+$ 140, HEPES 10.0, $CaCl_2$ 1.8, $MgCl_2$ 1.0, glucose 10.0, pH = 7.35 with HCl. Recording of gating currents was started only after disappearance of all voltage-dependent ionic current (40 mV) due to dialysis of the cell. The experiments were performed at room temperature.

For measurement of ionic currents the holding potential was generally –100 mV. The individual pulse protocols are described in the Results part. Small linear leakages and capacitive transients were removed by subtracting scaled averages of between 4 and 8 current traces elicited by pulses to –80 mV. The data were re-filtered with a Gaussian filter routine implemented in the ISO2 software at a cut-off frequency of 5 kHz.

Figure 1 shows examples of normalized current recordings of Kv1.2 and Kv2.1 channels expressed in CHO cells at the voltages of 0 and 40 mV. Kv1.2 channels activated significantly faster than Kv2.1 channels. Similar current time courses were obtained in L-cells (*not shown*). Statistically, the time interval between the clamp step and the half amplitude of the current ($t_{a,1/2}$) was indistin-

guishable between the two expression systems (Kv1.2, 0 mV, CHO cells 10.3 ± 0.6 ms ($n$ = 4), L-cells 9.0 ± 1.8 ms ($n$ = 10); 40 mV, CHO cells 2.5 ± 0.2 ms ($n$ = 4), L-cells 3.2 ± 0.5 ms ($n$ = 10); Kv2.1, 0 mV, CHO cells 21.5 ± 1.8 ms ($n$ = 9), L-cells 27.8 ± 2.8 ms ($n$ = 4); 40 mV, CHO cells 9.8 ± 0.7 ms ($n$ = 9), L-cells 10.7 ± 1.2 ms ($n$ = 4)). Hence the results in both cell lines were lumped.

For measurement of gating currents the holding potential was set to −100 mV (Kv2.1) or −120 mV (Kv1.2). Depolarizing pulses were elicited to voltages between −80 and 80 mV, spaced 10 or 5 mV. Capacitive and small linear leakage currents were removed by subtracting scaled averages of between 4 and 8 current traces elicited by pulses to −80 mV. In order to improve the signal-to-noise ratio, between 4 and 8 gating currents were averaged and the data were refiltered with a Gaussian filter routine at a cut-off frequency of 5 kHz.

### Fitting and Statistics

Various functions were fitted to the data points using the chi-square method of Origin 6.1 or the routines implemented in the ISO2 software. Statistical data are presented as mean ± SEM. Statistical significance was tested with Student's $t$-test ($P < 0.05$).

## Results

### Steady-State Activation

Under steady-state conditions two kinds of equivalent charge $z_g$ and $z_i$ can be measured: $z_g$ is determined from the gating current and reflects rearrangements of the gating machinery; $z_i$ is associated with the activation of the channel and can be determined from the ionic current. The measured equivalent charges do not need to be identical: $z_g$ can be larger than $z_i$ in the case that some channels do not open although they gate successfully. Alternatively, $z_g$ can be smaller than $z_i$. In this case, part of the gating charge that moves after the measurable gating current is completed, is too small to be detectable.

We determined $z_i$ from the amplitude of the tail currents (Fig. 2*A*) as described previously (Scholle et al., 2000). Amplitudes of instantaneous currents were normalized with respect to the maximum instantaneous current amplitude and plotted as function of voltage (Fig. 2*B*). The current-voltage relationship was fitted with a Boltzmann function according to

$$I_{rel}(V) = 1/\left\{1 + \exp\left[\left(V_{i,1/2} - V\right)z_i F/RT\right]\right\}^4 \qquad (1)$$

yielding the midpoint voltage $V_{i,1/2}$ of half-maximum activation and the equivalent charge $z_i$. $R$ is the molar gas constant, $T$ the absolute temperature in $K$, and $F$ the Faraday constant. We chose the power 4 in the Boltzmann function because of the assumed tetrameric structure of voltage-dependent $K^+$ channels (MacKinnon, 1991; Liman et al., 1992). This implies that the conformational changes of the four subunits during activation are identical and independent, as was assumed by Hodgkin & Huxley (1952). It should be noted, however, that the power is not well determined. The data points could be similarly described with powers between 1 and 5 in the Boltzmann function. $V_{i,1/2}$ values were similar for both channels and the equivalent charge $z_i$ for Kv1.2 channels was larger than the one for Kv2.1 channels (Table 1). Taking into account the tetrameric character of the channels, activation of Kv1.2 channels was apparently completed with the movement of $4 \times 3.52 = 14.08$ positive charges in the outward direction, whereas the one of Kv2.1 channels was completed with the movement of only $4 \times 1.48 = 5.92$ positive charges. In addition we estimated the total equivalent charge $z_{ls}$ required for activation with the method of the "limiting slope" (Almers, 1978). The $z_{ls}$ associated with activation of all four subunits was estimated from the limiting slope of the semilogarithmic plot of the steady-state activation for $V \to -\infty$ by

$$z_{ls} = \lim_{V \to -\infty} \left\{ \frac{RT}{F} \frac{d(\ln\ I_{rel})}{dV} \right\} \qquad (2)$$

The symbols have the same meaning as in Eq. 1. The diagram in Fig. 2*C* shows an example of a linear fit for Kv1.2 channels. The $z_{ls}$ values for Kv1.2 channels (7.42 ± 0.89; $n$ = 7) were markedly larger than the ones for Kv2.1 channels (2.61 ± 0.28; $n$ = 8; $P$ = 0.0012). Though the $z_{ls}$ values were smaller than those determined with the Boltzmann fit for steady-state activation ($z_i \times 4$), their ratio was similar.

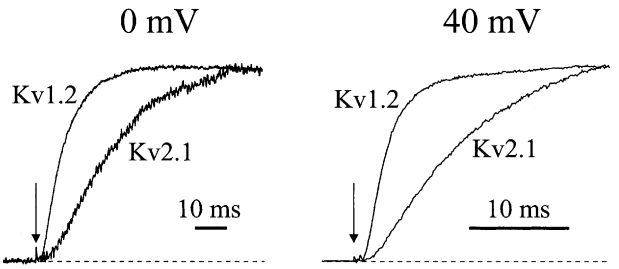


**Fig. 1.** Comparison of the activation time course of Kv1.2 and Kv2.1 channels at 0 and 40 mV. The amplitude of the current traces was scaled with respect to the late currents in the indicated time intervals. At both voltages, Kv2.1 channels activate with slower kinetics than do Kv1.2 channels.

### Gating Currents

Figure 3*A* shows examples of ON gating currents for both channels. To determine gating charge-voltage relations for these currents under steady-state conditions, they were integrated. Gating charges $Q$ were normalized with respect to the maximum gating charge $Q_{max}$ and the corresponding $Q_{rel}$ values were

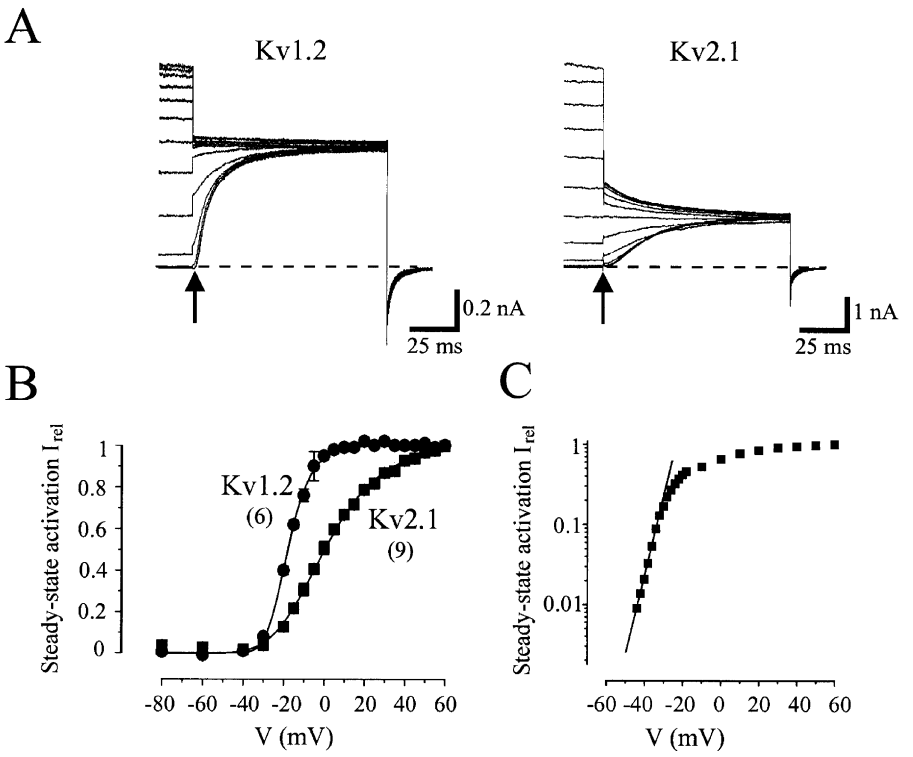


**Fig. 2.** Steady-state activation. (*A*) Representative current recordings as used to determine steady-state activation. The voltage protocol consisted of prepulses (200 ms) to the actual potential followed by test pulses (100 ms) to 0 mV. The instantaneous current 1 ms after the clamp step to the test pulse was evaluated (*arrows*). (*B*) Plot of the normalized instantaneous currents at 0 mV ($I_{rel}$) as function of the prepulse voltage. The curves are best fits with Eq 1. The parameters are shown in Table 1. Steady-state activation for Kv1.2 channels is steeper and at more negative voltages than that for Kv2.1 channels. Missing error bars indicate that SEM was smaller than the size of the symbols. (*C*) Semilogarithmic plot of steady-state activation $I_{rel}$ as function of voltage of a representative experiment of Kv1.2 channels. The slope of the line fitted to the data points at $I_{rel} < 0.032$ yields 5.55 for the total equivalent charge of activation of all subunits ($z_{ls}$; Eq 3.).

**Table 1.** Equivalent gating charges in steady-state relationships and activation time course

| Channel | Steady-state relationships | | | | | Forward transitions | | | |
|---|---|---|---|---|---|---|---|---|---|
| | $I_{rel}$ | | $Q_{rel}$ | | limiting slope | $\tau_g$ | $\tau_n$ | $t_{a,1/2}$ | $\tau_{al}$ |
| | $z_i$ | $V_{i,1/2}$ (mV) | $z_g$ | $V_{g,1/2}$ (mV) | $z_{ls}$ | $z_{gt}$ | $z_{del}$ | $z_{at}$ | $z_{al}$ |
| Kv1.2 | 3.52 | −30.0 | 1.91 | −21.42 | 7.42 | 0.65 | 0.76 | 1.66 | 2.12 |
| Kv2.1 | 1.48 | −28.55 | 2.42 | −20.99 | 2.61 | 0.62 | 0.86 | 0.94 | 1.31 |

$I_{rel}$ steady-state activation, fitted with Eq. 1, yielding the equivalent charge of the ionic current per subunit, $z_i$, and the voltage of half-maximum activation, $V_{i,1/2}$. $Q_{rel}$, normalized gating charge, fitted with Eq. 3, yielding the equivalent charge of the process producing the gating current, $z_g$, and the voltage of half-maximum charge movement, $V_{g,1/2}$. The limiting slope was determined with Eq. 2, as described in the text, yielding the total equivalent charge associated with activation of all four subunits, $z_{ls}$ . The error for $z_{ls}$ is indicated in the text. The equivalent charges of the gating current decay, $z_{gt}$, the ionic current delay, $z_{del}$, the half time of activation, $z_{at}$, and the late ionic current, $z_{al}$, were determined with Eq. 5 as described in the text. The number of cells included for each value corresponds to the numbers indicated in Figs. 2*B*, 3*B*, and 5, respectively.

plotted as function of test pulse voltage (Fig. 3*B*). The equation

$$Q_{rel}(V) = 1/\{1 + \exp[(V_{g,1/2} - V)z_g F/RT]\} \qquad (3)$$

was fitted to the data points yielding a midpoint voltage $V_{g,1/2}$ and an equivalent charge $z_g$ for the gating process of a single subunit. The results are summarized in Table 1. In the case of Kv1.2 channels, $z_g$ matched $z_{ls}$ ($4 \times z_g \approx z_{ls}$) but was significantly smaller than $z_i$. The results indicate that in Kv1.2 channels a fraction of gating charge is not detected in gating current and limiting slope measurements, most likely because this fraction of the gating charge only

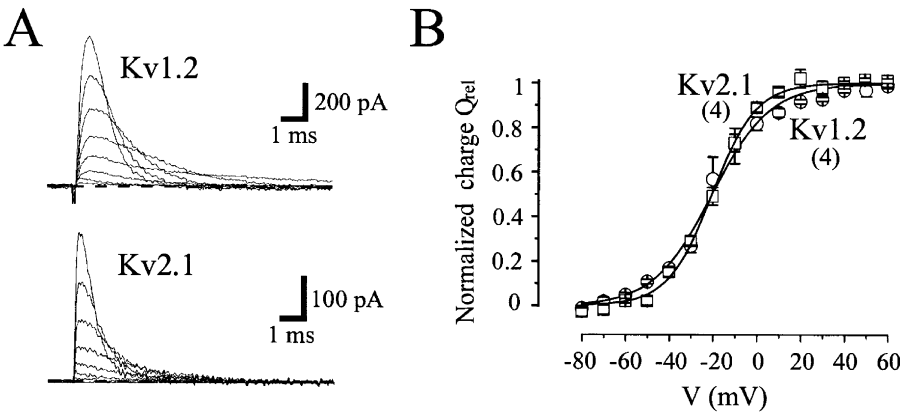


**Fig. 3.** ON gating currents and $Q$-$V$ relationships. (*A*) Representative recordings of ON gating currents. Test pulse potentials: −80, −60, −40, −20, 0, 20, 40, 60 mV. The traces shown are averages of 5 individual traces. (*D*) Charge versus voltage relationships $Q_{rel}(V)$ as obtained from the time integral of the gating currents and normalizing the values with respect to the value at 60 mV. The curves were best fits, with Eq. 3 yielding the parameters in Table 1. Missing error bars indicate that SEM was smaller than the size of the symbols.

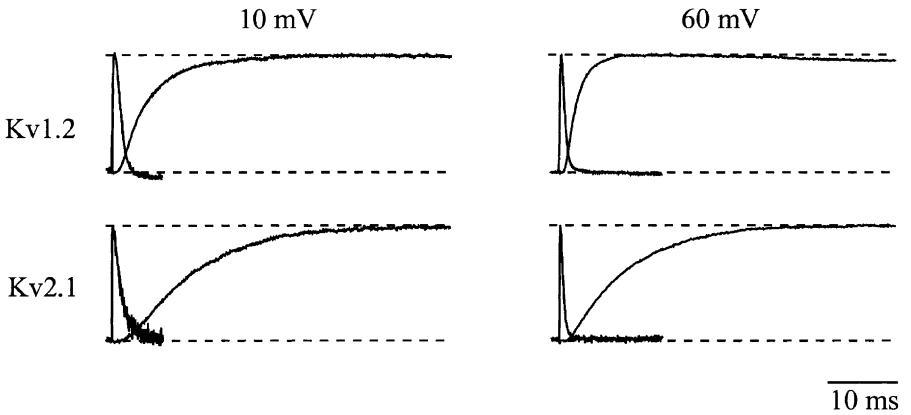


**Fig. 4.** Comparison of the time courses of the ON gating and the ionic current in Kv1.2, and Kv2.1 channels at 10 and 60 mV. The currents were normalized with respect to the maximum current during the test pulse of 200 ms duration. At the same voltage the time course of the gating currents is similar, whereas the ionic currents show the characteristic difference in the activation kinetics.

moves during the coupling of the gating to the pore opening. By contrast, only a fraction of the equivalent charge $z_g$ contributes to the activation of Kv2.1 channels, where $z_g$ markedly exceeds $z_{ls}$ ($4 \times z_g > z_{ls}$) and is even larger than $z_i$.

## Kinetic Parameters at Different Stages of the Activation Process

Inspection of representative ON gating currents suggested that their time course was similar for both channels over a wide voltage range (Fig. 3*A*) and comparison of time courses of ON gating and ionic currents at the same voltage (Fig. 4) directly suggest that the kinetics of gating charge movement recorded by the gating currents do not account for the differences seen in the activation time courses. Statistical analysis is provided below. Apparently, most of the gating charge has moved before the channels opened. Generally, the movement of the gating charge does not need to be restricted to the early movement of the gating machinery but may also take place at later stages of the activation process; i.e. the gating charge movement may spread over the whole activation process (Zagotta, Hoshi & Aldrich, 1994a). In order to gain information about the spreading of the gating charge upon activation, we determined the equivalent charges of four gating parameters characterizing unidirectional forward transitions during activation. Since the equivalent charges that determine the transition rates from one state to another state correspond only to the equivalent charges moved before the transition states, but not to the charges moved after the transition states (*cf.* Zagotta et al., 1994a), these equivalent charges can not be directly related to those determined under steady-state conditions.

ON gating currents, the earliest measure of channel activation, showed the typical short initial rising phase (Fig. 3*A*; *cf.* Bezanilla et al., 1991; Taglialatela & Stefani, 1993; Stefani et al., 1994; Wang et al., 1999). Since the rising phase was short compared to the activation time course of the ionic

**Table 2.** Contributions of a voltage-dependent component, $A$, and a voltage-independent component, $B$, to the time parameters $\tau_g$, $\tau_{del}$, $t_{a,1/2}$, and $\tau_{al}$ for activation as determined with Eq. 5.

| Time parameters | Kv1.2 | | | Kv2.1 | | |
|---|---|---|---|---|---|---|
| | $A$ (ms) | $B$ (ms) | $B/(A+B)$ | $A$ (ms) | $B$ (ms) | $B/(A+B)$ |
| $\tau_g$ | 2.38 | 0 | 0 | 2.92 | 0 | 0 |
| $\tau_n$ | 2.77 | 0.91 | 0.25 | 6.36 | 1.08 | 0.15 |
| $t_{a,1/2}$ | 8.28 | 2.47 | 0.23 | 15.19 | 6.21 | 0.29 |
| $\tau_{al}$ | 20.73 | 2.77 | 0.12 | 13.39 | 8.17 | 0.38 |

The term $[B/(A+B)]$ indicates the relative contribution of the voltage-independent component. The number of cells included for each value corresponds to the numbers indicated in Fig. 5.

current and not well resolved in our whole-cell recordings, it was not considered in the further analysis and a monoexponential function

$$I = I_0 \exp(-t/\tau_{gt}) \tag{4}$$

was fitted to the decay time course (Fig. 5*Aa*; *see* also Zagotta et al., 1994a). $I_0$ is an amplitude parameter, $t$ the time, and $\tau_{gt}$ the decay time constant. The equivalent charge $z_{gt}$ of gating current relaxation was obtained by fitting a plot of $\tau_{gt}$ values versus voltage using equation (5). This equation was generally used to describe the voltage dependency of time parameters.

$$\tau = A \exp(-z_x FV/RT) + B. \tag{5}$$

$A$ and $B$ are amplitude parameters of a voltage-dependent and voltage-independent component, respectively. Equation (5) was fitted to the plots $\tau_{gt}$ *versus* $V$ between 0 and 60 mV (Fig. 5*Ab*). $B$ was set to zero and $z_x$ was $z_{gt}$. The calculated $z_{gt}$ values are summarized in Table 1. The main conclusion from these data is that forward transitions of the reactions generating the Kv1.2 gating currents covered only a relatively small fraction of the total equivalent charge determined for the ionic current ($z_{gt}/z_i = 0.18$), whereas the respective value for Kv2.1 channels was larger ($z_{gt}/z_i = 0.42$).

The total activation time course of the ionic current could not be described by Hodgkin-Huxley (HH)-type models (powers 2 to 6 tested; Hodgkin & Huxley, 1952). In order to quantify the voltage dependence of the initial activation time course, we fitted the initial sigmoidal activation time course between point zero and the inflection point by the HH model

$$I = I_\infty[1 - \exp(-t/\tau_n)]^4. \tag{6}$$

$I_\infty$ is an amplitude parameter of the theoretical current $I$ at $t \to \infty$ and $\tau_n$ is the time constant of activation of a single subunit. The resulting time constant $\tau_n$ was plotted as function of voltage (Fig. 5*Bb*) and the equivalent charge of the initial activation time course of a single subunit $z_{del}$ ('del' for 'delay'), was calculated from Eq. 5 with $z_{del} = z_x$. The parameter $B$ could not be fixed to zero (*see* Table 2). Though the values of $z_{del}$ were similar for both channels (0.76 and 0.86 per subunit or 3.04 and 3.44 per channel, respectively; Table 1), the sigmoidal activation time course of the initial ionic current was already slower in Kv2.1 than in Kv1.2 channels.

The time interval between the beginning of the test pulse and the half amplitude of the current, $t_{a,1/2}$, was considered a third parameter to describe the sequence of forward transitions during activation (Fig. 5*Ca*). This time interval should include later forward transitions than those described by $\tau_n$ because the inflection point, used as end point of the time interval for determining $\tau_n$, occurred earlier than the time point of half-maximum current amplitude. The $t_{a,1/2}$ values refer to the activation of the whole channel and not to the one of a single subunit. Measured $t_{a,1/2}$ values were plotted as function of voltage (Fig. 5*Cb*). In contrast to $\tau_n$, the $t_{a,1/2}$ values for both channels differed more at 60 mV than at −10 mV, indicative of a different voltage dependence of the processes determining the initial and the later channel activation. Fits of Eq. 5 to the data yielded the equivalent charge for the half time of activation $z_{at} = z_x$. The values of $z_{at}$ and the amplitude parameters are summarized in Tables 1 and 2, respectively.

In sequential kinetic models the late activation time course will be dominated by the slowest forward rate constant if the backward reactions are negligible. This should be the case at sufficiently depolarized voltages (*see* Zagotta et al., 1994a). We fitted equation 7 to the late activation time course, beginning at the half maximum current (Fig. 5*Da*).

$$I = I_\infty[1 - 0.5 \exp(-t/\tau_{al})] \tag{7}$$

where $\tau_{al}$ is the activation time constant and $I_\infty$ the amplitude of the late current. The $\tau_{al}$ values were plotted as function of voltage. Noticeably, the $\tau_{al}$ relationships crossed each other: due to a steeper voltage dependence of $\tau_{al}$ in Kv1.2 than in Kv2.1 channels, late activation for Kv2.1 channels was only slower at strong depolarization (> 20 mV).

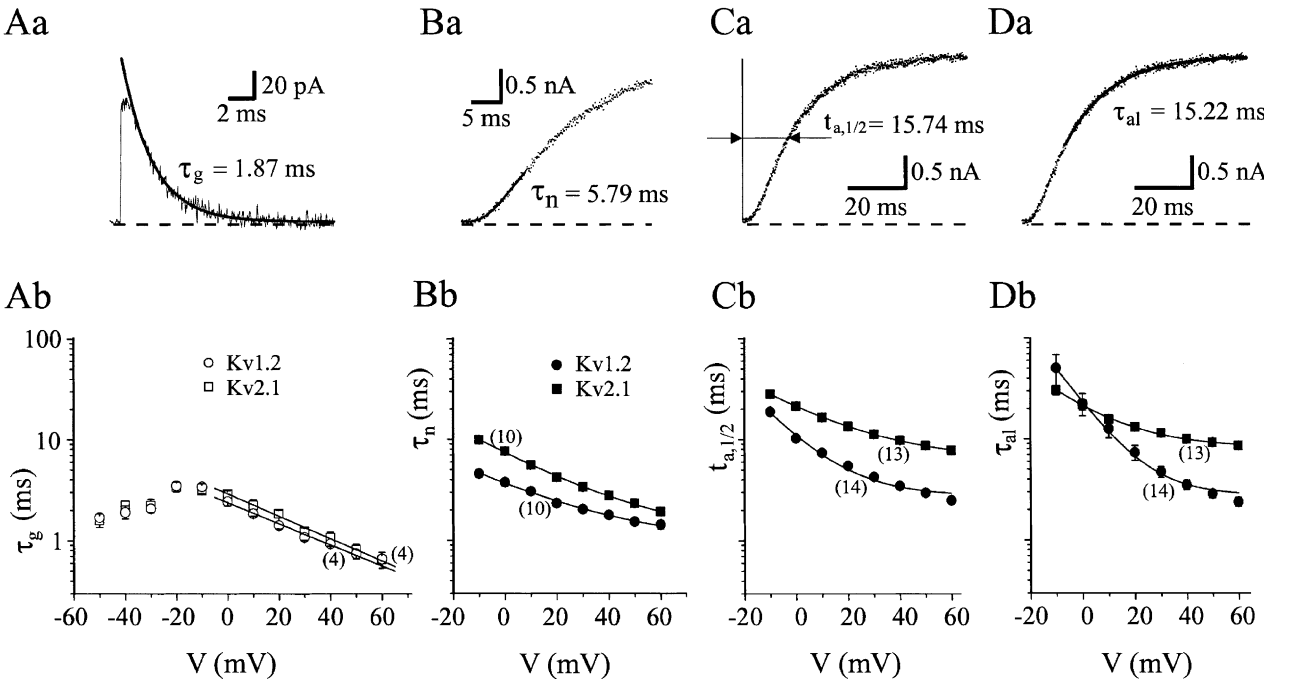


**Fig. 5.** Voltage dependence of activation parameters for Kv1.2 and Kv2.1 channels. (*A*) Gating current decay. (*Aa*) Example of a Kv2.1 gating current at 10 mV. The decay phase is described, with Eq. 4 yielding the time constant $\tau_{gt}$. (*Ab*) Plot of the decay time constant $\tau_{gt}$ as function of voltage on a semilogarithmic scale. Equation 5 was fitted to the data points with $z_{gt} = z_x$. The values of $z_{gt}$ are given in Table 1. (*B*) Initial time course of activation of the ionic current. (*Ba*) Example of a Kv2.1 current. Test-pulse voltage 10 mV. Equation 6 was fitted to the initial part of the ionic current until the inflection point yielding the activation time constant $\tau_n$. (*Bb*) Plot of the activation time constant $\tau_n$ as function of voltage on a semilogarithmic scale. Equation 5 was fitted to the data points, with $z_{del} = z_x$. The $z_{del}$ values are given in Table 1. (*C*) Time interval between clamp step and half-maximum activation of the ionic current, $t_{a,1/2}$. (*Ca*) Example of an ionic current recorded from Kv2.1 channels, showing the method of determination of $t_{a,1/2}$. Same current as in *Ba*. (*Cb*) Plot of $t_{a,1/2}$ as function of voltage on a semilogarithmic scale. Equation 5 was fitted to the data points, with $z_{al} = z_x$. The $z_{al}$ values are given in Table 1. (*D*) Late time course of activation of the ionic current. (*Da*) Example of an ionic current recorded from Kv2.1 channels expressed in CHO cells. Same current as in *Ba*. Equation 7 was fitted to the time interval of the late ionic current, starting from the half maximum amplitude, yielding the time constant of late activation $\tau_{al}$. (*Db*) Plot of the late activation time constant $\tau_{al}$ as function of voltage on a semilogarithmic scale. Equation 5 was fitted to the data points, with $z_{al} = z_x$. The $z_{al}$ values are given in Table 1.

Equation 5 was fitted to the plots in order to determine the equivalent charge of the late ionic current activation $z_{al} = z_x$ (Fig. 5*Db*). Parameter *B* was unequal zero for both channels (*see* Table 2). The respective $z_{al}$ values are summarized in Table 1. The results showed that forward transitions determining the late activation time course were voltage dependent for both channels and that the voltage dependence was nearly twice as steep for Kv1.2 than for Kv2.1 channels.

## The Sigmoidicity of Activation Is Differently Voltage Dependent in Kv1.2 and Kv2.1 Channels

Sigmoidicity of the activation time course can be defined as the amount of delay relative to the overall rate of activation (Zagotta et al., 1994a). If assuming that a number of first-order transitions in independent subunits rate-limit the activation time course, the sigmoidicity would be the same at each voltage. In contrast, if the concerted coupling reaction, following the subunit gating, rate-limits the activation time course, the sigmoidicity would be reduced. As reported by Zagotta and coworkers (1994a), a simple method to compare sigmoidicity of the activation time course at different voltages is to first scale the currents with respect to the steady-state amplitude and then adjust the time expansion to a similar rate of rise at half-maximum current. Figure 6 shows representative examples of traces for both channels after such a normalization in both amplitude and time. As reference served the currents at 60 mV. Kv2.1 channels produced an approximately similar sigmoidicity at all voltages, with a slightly larger sigmoidicity at −10 mV than at 60 mV. In contrast, the sigmoidicity for Kv1.2 channels was much more voltage dependent and oppositely directed: it was most pronounced at 60 mV and least pronounced at −20 mV. The conclusion is that rate limitation of the activation process in the two channels is differently controlled (*see* Discussion).

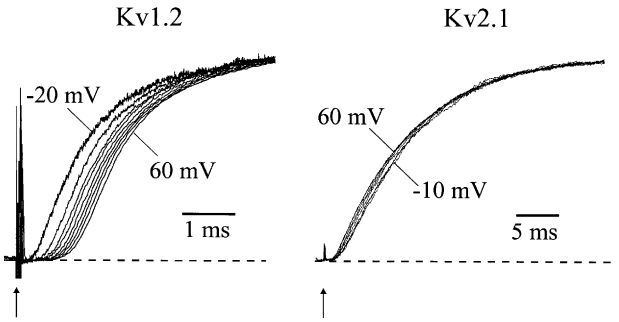


**Fig. 6.** Sigmoidicity of the activation time course in Kv1.2 and Kv2.1 channels. The currents were scaled in amplitude with respect to the late current and in time with respect to slope at the half amplitude. In Kv2.1 channels the traces at −10 and 0 mV were re-filtered to 1 kHz to reduce the noise. Time calibration is valid for the reference currents at 60 mV only. Kv1.2: test pulse voltages −20 mV through 60 mV; Kv2.1: −10 mV through 60 mV in 10 mV increments each; pulse duration and pulsing frequency 200 ms and 0.5 Hz, respectively. The sigmoidicity was steeply voltage dependent for Kv1.2 channels, with a maximum at strong depolarization, whereas it was only weakly voltage dependent for Kv2.1 channels with a maximum at moderate depolarization. For further explanation *see* text.

## Discussion

Kv1.2 channel gating can be described by the scheme

$$(C_1 \underset{k_1}{\rightarrow} C_2)_4 \underset{k_2}{\rightarrow} O. \qquad \text{Scheme (1)}$$

The scheme is given in an abbreviated format (Zagotta, Hoshi & Aldrich, 1994b). *C*'s are closed states of independently gating subunits, *O* is the open state, $k_1$ and $k_2$ describe rates of forward reactions (in the direction of activation). The rate constant $k_1$ describes the independent gating of the subunits and mainly reflects the gating current kinetics. The short rising phase of the gating currents is not separately considered and thus included in $k_1$. The rate constant $k_2$ describes the concerted coupling reaction. It significantly accounts for the late (exponential) activation time course ($\tau_{al}$). Since all three time constants, $\tau_g$, $\tau_n$, $\tau_{al}$ decrease at stronger depolarization, it is assumed that $k_1$ and $k_2$ accelerate at stronger depolarization. A different contribution of $k_1$ and $k_2$ to rate limitation at different voltages can then be explained by different voltage dependencies of the rates. The sigmoidicity of Kv1.2 currents was more pronounced at strong rather than moderate depolarization (Fig. 6). Since all models with any number of independent first-order transitions produce identical sigmoidicity (Zagotta et al., 1994a), this result suggests that the activation of Kv1.2 channels is not preferentially rate-limited by the gating of independent subunits over the whole tested voltage range but also by the subsequent coupling reaction: At moderate depolarization the coupling reaction ($k_2$) would contribute more to the rate limitation of the activation process than at strong depolarization where rate limitation is more influenced by the subunit gating. Since the total time course of activation accelerates upon depolarization, $k_1$ *and* $k_2$ would accelerate, but $k_2$ more than $k_1$. Involvement of the coupling reaction ($k_2$) in rate limitation even at the strongest depolarization arises from the result that the activation of the ionic current was still slower than the gating current decay (*cf.* Fig. 4).

For Kv2.1 channels the model should explain (1) that the channels activate more slowly than Kv1.2 channels, (2) that the sigmoidicity is only weakly voltage-dependent, and (3) that the gating currents are as fast as in Kv1.2 channels. The combination of points (1) and (3) requires that larger rate limitation than in Kv1.2 channels arises in processes following the reactions generating the gating currents. The fact that the sigmoidicity is only weakly voltage-dependent (2) suggests that an essential portion of rate limitation in the Kv2.1 channel gating is included in the independent transitions of the subunits (*see* above). The gating scheme is therefore extended by an additional reaction in the subunit gating ($k_1'$) to

$$(C_1 \underset{k_1}{\rightarrow} C_2 \underset{k_1'}{\rightarrow} C_3)_4 \underset{k_2}{\rightarrow} O \qquad \text{Scheme (2)}$$

and our results suggest that at all voltages the main rate limitation is caused by $k_1'$. The moderate and oppositely directed voltage dependence of the sigmoidicity in Kv2.1 channels (Fig. 6) with respect to Kv1.2 channels can be explained by assuming that $k_1'$ decreases somewhat more at depolarization than does $k_2$. In summary, in Kv2.1 channels depolarization induces acceleration of activation mainly via a reaction in the subunit gating following movement of the voltage sensor, whereas in Kv1.2 channels the main acceleration of activation is caused by the coupling reaction, thereby increasing the rate-limiting influence of the subunit gating. Taking into account that the slower activation in Kv2.1 channels is caused by the S4 segment, the S5-pore linker and the pore itself (Scholle et al., 2000; *see* also for sequence alignment), these three regions may be suggested to contribute mainly to rate-limiting reactions in the subunit movement and not in the coupling reaction.

These interpretations fit with the observation that the time constant for the late activation, $\tau_{al}$, depended more steeply on voltage for Kv1.2 than for Kv2.1 channels. When considering the two components contributing to $\tau_{al}$, the analysis showed that this was due to both a stronger influence of the voltage-dependent component *A* (20.73 versus 13.39 ms) and a three times smaller voltage-independent component *B* compared to Kv2.1 channels (2.77 versus 8.17 ms). At strong depolarization it is particularly the faster voltage-independent component *B* that allows for the faster activation in Kv1.2 compared to Kv2.1 channels. The key role of a voltage-independent reaction

for the different late activation time courses of the two channels can also be derived by comparing $[B/(A + B)]$ along the three measured time parameters: $[B/(A + B)]$ decreased from the initial ($\tau_n$) to the late time course ($\tau_{al}$) in Kv1.2 channels ($0.25 \rightarrow 0.12$), whereas it increased in Kv2.1 channels ($0.15 \rightarrow 0.38$). The conclusion is that at strong depolarization the time course of activation in Kv2.1 versus Kv1.2 channels is obstructed by a voltage-independent reaction. If $k_1'$ in Scheme (2) is rate limiting in Kv2.1 channels then it would not simply change according to an exponential function of voltage but would approximate a maximum.

When comparing the $I_{rel}$ (V) relationship determined for Kv1.2 channels with the relationships for the best studied channel of the Kv1 family, the *Shaker* channel with removed N-type inactivation (*Shaker* Δ6-46), Perozo and co-workers (1994) observed a similar voltage dependence (Zagotta et al., 1994a). Hence, steady-state activation of the ionic current is similar in rat Kv1.2 and *Shaker* Δ6-46 channels. By contrast, the $Q_{rel}$ ($V$) relationship in Kv1.2 channels was shifted by 20 to 30 mV to more positive potentials with respect to *Shaker* Δ6-46 (Zagotta et al., 1994a; Perozo et al., 1994) and the equivalent charge of the gating process $z_g$ was smaller in Kv1.2 channels than in *Shaker* Δ6-46 channels (1.91 versus 3.6). These differences indicate a difference in the gating between both channels. Basically similar to *Shaker* Δ6-46 channels is that in all channels studied herein a portion of the gating charge was found to move only during the activation of the ionic current, i.e., much later than measurable with the gating current. When comparing the $z$ values determined for the activation of Kv1.2 channels (Table 1) with corresponding values of *Shaker* Δ6-46 channels (Zagotta et al., 1994a), the most striking difference exists in the late activation ($\tau_{al}$): In Kv1.2 channels the equivalent charge of the late ionic current, $z_{al}$, was approximately five times larger than that in *Shaker* Δ6-46 channels (2.11 versus 0.42). The slow component of activation was present until the strongest depolarizations studied herein and it prevented the use of Hodgkin-Huxley-type models for description.

For Kv2.1 channels, Taglialatela and Stefani (1993) reported that the time constant, obtained from fitting the activation time course with a single exponential, matches the decay time constant, obtained from fitting the decay phase of the gating current (denoted $\tau_g$ herein). The result suggested that the kinetics of the gating current directly control the activation kinetics of the ionic current. In contrast, our results show that at all voltages the gating current decay for Kv2.1 channels is faster than the activation of the ionic current (Fig. 4). Thus, our results imply that the kinetics of the gating current do not directly control the activation kinetics of the ionic current and that an additional rate-limiting reaction must occur in-between ($k_2$ in Scheme 1). One reason for the different time relation between gating and ionic current of our results and those of Taglialatela and Stefani (1993) might arise from different recording techniques (cut-open oocytes versus whole-cell recording in cultured cells). Another possibility might arise from different properties of rat Kv2.1 channels they used and human Kv2.1 channels used herein, because rat channels activate about twice as fast than human channels (Ju et al., 2003).

## Conclusions

The similarity of the ON gating current kinetics implies that the early molecular arrangements of the activation gating are similar in Kvl.2 and Kv2.1 channels, suggesting that the voltage sensors move with similar kinetics through the phospholipid membrane. The differences in the activation kinetics between the two channels are inferred by subsequent rate-limiting reactions in the activation process: In Kv1.2 channels the coupling reaction contributes to rate limitation at moderate depolarization but reduces its effect at strong depolarization. In contrast, activation of Kv2.1 channels is rate-limited at all voltages by an additional slow reaction in the subunit gating.

We thank Dr. T. Baukrowitz for helpful comments on an earlier version of the manuscript and S. Bernhardt, A. Kolchmeier, K. Schoknecht, and B. Tietsch for excellent technical assistance. This work was supported by grant Bel250/4-3 of the Deutsche Forschungsgemeinschaft to K.B.

## References

Aggarwal, S.K., MacKinnon, R. 1996. Contribution of the S4 segment to gating charge in the *Shaker* $K^+$ channel. *Neuron* **16:**1169–1177

Almers, W. 1978. Gating currents and charge movements in excitable membranes. *Rev. Physiol. Biochem. Pharmacol.* **82:**96–190

Bezanilla, F. 2000. The voltage sensor in voltage-dependent ion channels. *Physiol. Rev.* **80:**555–592

Bezanilla, F., Perozo, E., Papazian, D.M., Stefani, E. 1991. Molecular basis of gating charge immobilization in *Shaker* potassium channels. *Science* **245:**679–683

Cha, A., Bezanilla, F. 1997. Characterizing voltage-dependent conformational changes in the *Shaker* $K^+$ channel with fluorescence. *Neuron* **19:**1127–1140

Cha, A., Bezanilla, F. 1998. Structural implications of fluorescence quenching in the *Shaker* $K^+$ channel. *J. Gen. Physiol.* **112:**391–408

Chen, J., Mitcheson, J.S., Tristani-Firouzi, M., Lin, M., Sanguinetti, M.C. 2001. The S4-S5 linker couples voltage sensing and activation of pacemaker channels. *Proc. Natl. Acad. Sci. USA* **98:**11277–11282

Cohen, B.E., Grabe, M. 2003. Answers and questions from the KvAP structures. *Neuron* **39:**395–400

Elinder, F., Manniko, R., Larsson, H.P. 2001. S4 charges move close to residues in the pore domain during activation a potassium channel. *J. Gen. Physiol.* **118:**1–10

Heginbotham, L., MacKinnon, R. 1992. The aromatic binding site for tetraethylammonium ion on potassium channels. *Neuron* **8:**483–491

Hodgkin, A.L., Huxley, A.F. 1952. A quantitative description of the membrane current and its application to conduction and excitation in nerve. *J. Physiol.* **117:**500–544

Jiang, Y., Lee, A., Chen, J., Ruta, V., Cadene, M., Chait, B.T., MacKinnon, R. 2003a. X-ray structure of a voltage-dependent $K^+$ channel. *Nature* **423:**33–41

Jiang, Y., Ruta, V., Chen, J., Lee, A., MacKinnon, R. 2003b. The principle of gating charge movement in a voltage-dependent $K^+$ channel. *Nature* **423:**42–48

Ju, M., Stevens, L., Leadbitter, E., Wray, D. 2003. The roles of N- and C-terminal determinants in the activation of the Kv2.1 potassium channel. *J. Biol. Chem.* **278:**12769–12778

Koopmann, R., Scholle, A., Ludwig, J., Leicher, T., Zimmer, T., Pongs, O., Benndorf, K. 2001. Role of the S2 and S3 segment in determining the activation kinetics in Kv2.1 channels. *J. Membrane Biol.* **182:**49–59

Larsson, H.P., Baker, O.S., Dhillon, D.S., Isacoff, E.Y. 1996. Transmembrane movement of the *Shaker* $K^+$ channel S4. *Neuron* **16:**387–397

Liman, E.R., Hess, P., Weaver, F., Koren, G. 1991. Voltage-sensing residues in the S4 region of a mammalian $K^+$ channel. *Nature* **353:**752–756

Liman, E.R., Tytgat, J., Hess, P. 1992. Subunit stoichiometry of a mammalian $K^+$ channel determined by construction of multimeric cDNAs. *Neuron* **9:**861–871

Logothetis, D.E., Movahedi, S., Satler, C., Lindpaintner, K., Nadal-Ginard, B. 1992. Incremental reductions of positive charge within the S4 region of a voltage-gated $K^+$ channel result in corresponding decreases in gating charge. *Neuron* **8:**531–540

MacKinnon, R. 1991. Determination of the subunit stoichiometry of a voltage-activated potassium channel. *Nature* **350:**232–235

McCormack, K., Tannouye, M.A., Iverson, L.E., Lin, J-W., Ramaswami, M., McCormack, T., Campanelli, J.T., Mathew, M.K., Rudy, B. 1991. A role for hydrophobic residues in the voltage-dependent gating of *Shaker* $K^+$ channels. *Proc. Natl. Acad. Sci. USA* **88:**2931–2935

Milligan, C.J., Wray, D. 2000. Local movement in the S2 region of the voltage-gated potassium channel hKv2.1 studied using cysteine mutagenesis. *Biophys. J.* **78:**1852–1861

Papazian, D.M., Shao, X.M., Seoh, S.A., Mock, A.F., Huang, Y., Wainstock, H.D. 1995. Electrostatic interactions of S4 voltage sensor in *Shaker* $K^+$ channel. *Neuron* **14:**1293–1301

Papazian, D.M., Timpe, L.C., Jan, Y.N., Jan, L.Y. 1991. Alteration of voltage-dependence of *Shaker* potassium channel by mutations in the S4 sequence. *Nature* **349:**305–310

Perozo, E., Santacruz Toloza, L., Stefani, E., Bezanilla, F., Papazian, D.M. 1994. S4 mutations alter gating currents of *Shaker* K channels. *Biophys. J.* **66:**345–354

Planells-Cases, R., Ferrer Montiel, A.V., Patten, C.D., Montal, M. 1995. Mutation of conserved negatively charged residues in the S2 and S3 transmembrane segments of a mammalian $K^+$ channel selectively modulates channel gating. *Proc. Natl. Acad. Sci. USA* **92:**9422–9426

Sanguinetti, M.C., Xu, Q.P. 1999. Mutations of the S4-S5 linker alter activation properties of HERG potassium channels expressed in *Xenopus* oocytes. *J. Physiol.* **514:**667–675

Scholle, A., Koopmann, R., Leicher, T., Ludwig, J., Pongs, O., Benndorf, K. 2000. Structural elements determining activation kinetics in Kv2.1. *Recept. Channels* **7:**65–75

Seoh, S.A., Sigg, D., Papazian, D.M., Bezanilla, F. 1996. Voltage-sensing residues in the S2 and S4 segments of the *Shaker* $K^+$ channel. *Neuron* **16:**1159–1167

Shieh, C.-C., Klemig, K.G., Kirsch, G.E. 1997. Role of transmembrane segment S5 on gating of voltage-dependent $K^+$ channels. *J. Gen. Physiol.* **109:**767–778

Starace, D.M., Stefani, E., Bezanilla, F. 1997. Voltage-dependent proton transport by the voltage sensor of the *Shaker* $K^+$ channel. *Neuron* **19:**1319–1327

Stefani, E., Toro, L., Perozo, E., Bezanilla, F. 1994. Gating of *Shaker* channels I. Ionic and gating currents. *Biophys. J.* **66:**996–1010

Taglialatela, M., Stefani, E. 1993. Gating currents of the cloned delayed-rectifier $K^+$ channel DRK1. *Proc. Natl. Acad. Sci. USA.* **90:**4758–4762

Tiwari Woodruff, S.K., Schulteis, C.T., Mock, A.F., Papazian, D.M. 1997. Electrostatic interactions between transmembrane segments mediate folding of *Shaker* $K^+$ channel subunits. *Biophys. J.* **72:**1489–1500

Tristani-Firouzi, M., Chen, J., Sanguinetti, M.C. 2002. Interactions between S4-S5 linker and S6 transmembrane domain modulate gating of HERG $K^+$ channels. *J. Biol. Chem.* **277:**18994–19000

Yellen, G. 2002. The voltage-gated potassium channels and their relatives. *Nature.* **419:**35–42

Yusaf, S.P., Wray, D., Sivaprasadarao, A. 1996. Measurement of the movement of the S4 segment during the activation of a voltage-gated potassium channel. *Pfluegers Arch.* **433:**91–97

Wang, Z., Zhang, X., Fedida, D. 1999. Gating current studies reveal both intra- and extracellular cation modulation of $K^+$ channel deactivation. *J. Physiol.* **515:**331–339

Zagotta, W.N., Hoshi, T., Aldrich, R.W. 1994a. *Shaker* potassium channel gating. II: Transitions in the activation pathway. *J. Gen. Physiol.* **103:**279–319

Zagotta, W.N., Hoshi, T., Aldrich, R.W. 1994b. *Shaker* potassium channel gating. III: Evaluation of kinetic models for activation. *J. Gen. Physiol.* **103:**321–362